Interaction between Raphidiopsis raciborskii and rare bacterial species revealed by dilution-to-extinction experiments

Article *in* Harmful Algae · November 2022

DOI: 10.1016/j.hal.2022.102350

CITATIONS
0

READS
8

9 authors, including:

Jun Zuo
Chinese Academy of Sciences
11 PUBLICATIONS **41** CITATIONS
SEE PROFILE

Fengjiao Tan
Institue of Urban Environment, CAS
3 PUBLICATIONS **8** CITATIONS
SEE PROFILE

Hongteng Zhang
Chinese Academy of Sciences
1 PUBLICATION **1** CITATION
SEE PROFILE

Xue Yuanyuan
Chinese Academy of Sciences
21 PUBLICATIONS **569** CITATIONS
SEE PROFILE

Harmful Algae 120 (2022) 102350

Contents lists available at ScienceDirect

Harmful Algae

journal homepage: www.elsevier.com/locate/hal

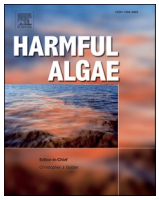

Interaction between *Raphidiopsis raciborskii* and rare bacterial species revealed by dilution-to-extinction experiments

Jun Zuo [a], Fengjiao Tan [a,b], Hongteng Zhang [a,b], Yuanyuan Xue [a], Hans-Peter Grossart [c,d], Erik Jeppesen [e,f,g,h], Peng Xiao [a,i], Huihuang Chen [a,b], Jun Yang [a,*]

[a] *Aquatic EcoHealth Group, Fujian Key Laboratory of Watershed Ecology, Key Laboratory of Urban Environment and Health, Institute of Urban Environment, Chinese Academy of Sciences, Xiamen 361021, China*
[b] *University of Chinese Academy of Sciences, Beijing 100049, China*
[c] *Leibniz-Institute of Freshwater Ecology and Inland Fisheries (IGB), Stechlin 16775, Germany*
[d] *University of Potsdam, Institute of Biochemistry and Biology, Potsdam 14469, Germany*
[e] *Department of Ecoscience, Aarhus University, Aarhus 8000, Denmark*
[f] *Sino-Danish Centre for Education and Research, Beijing 100049, China*
[g] *Limnology Laboratory, Department of Biological Sciences and Centre for Ecosystem Research and Implementation, Middle East Technical University, Ankara 06800, Turkey*
[h] *Institute of Marine Sciences, Middle East Technical University, Mersin 33731, Turkey*
[i] *National and Local Joint Engineering Research Center of Ecological Treatment Technology for Urban Water Pollution, College of Life and Environmental Science, Wenzhou University, Wenzhou 325035, China*

ARTICLE INFO

Editor Dr. C. Gobler

Keywords:
Plankton
Species interaction
Rare species
Raphidiopsis
Harmful cyanobacterial bloom
Algae-bacteria relationship

ABSTRACT

Interactions between heterotrophic bacteria and cyanobacteria regulate the structure and function of aquatic ecosystems and are thus crucial for the prediction and management of cyanobacterial blooms in relation to water security. Currently, abundant bacterial species are of primary concern, while the role of more diverse and copious rare species remains largely unknown. Using a dilution-to-extinction approach, rare bacterial species from reservoir water were co-cultured with the bloom-forming cyanobacterium *Raphidiopsis raciborskii* in the lab to explore their interactions by using Phyto-PAM and 16S rRNA gene high-throughput sequencing. We found that a ≤1000-fold bacterial dilution led to bacteria control of the growth and photosynthesis of *R. raciborskii*. Moreover, the bacterial community compositions in the low-dilution groups were clearly diverged from the high-dilution groups. Importantly, rare species changed dramatically in the low-dilution groups, resulting in lower phylogenetic diversity and narrower niche width. The network complexity and compositional stability of bacterial communities decreased in the low-dilution groups. Collectively, our results suggest that rare bacterial species inhibit *R. raciborskii* growth and photosynthesis through microbial interactions mediated by species coexistence and interaction mechanisms. Our study provides new knowledge of the ecological role of rare bacteria and offers new perspectives for understanding the outbreak and regression of *R. raciborskii* blooms.

1. Introduction

Heterotrophic bacteria play a substantial role in the global biogeochemical cycling of carbon (C), nitrogen (N), phosphorus (P) and sulphur (S) elements in aquatic ecosystems (Gao et al., 2021; Li et al., 2021a; Raymond et al., 2013; Stegen et al., 2016). They can interact with cyanobacteria, benefit from associations with cyanobacteria and also affect the cyanobacterial bloom biomass (abundance and composition) (Huisman et al., 2018; Seymour et al., 2017; Te et al., 2017) and their toxicity (Dziallas and Grossart, 2011a; Vico et al., 2021; Woodhouse et al., 2016; Zhu et al., 2016). Harmful cyanobacterial blooms are an increasing problem worldwide due to global warming and anthropogenic activities (Ho et al., 2019; Paerl and Huisman, 2008). While current research efforts often focus on abiotic factors, such as N/P nutrition, light, reactive oxygen radicals, temperature and hydrometeorology (Dziallas and Grossart, 2011b; Wilhelm et al., 2020; Yang et al., 2017), biotic factors are less well studied (Cook et al., 2020; Herren and McMahon, 2018; Huisman et al., 2018; Seymour et al., 2017; Vico et al.,

* Corresponding author.
E-mail address: jyang@iue.ac.cn (J. Yang).

https://doi.org/10.1016/j.hal.2022.102350
Received 10 April 2022; Received in revised form 31 October 2022; Accepted 6 November 2022
Available online 25 November 2022

2021; Zuo et al., 2021). A recent review by Dick et al. (2021) highlighted that cyanobacteria interactions with heterotrophic bacteria play a vital role in the dynamics of phytoplankton communities and the variations in the fitness of the phytoplankton host. Moreover, Vico et al. (2021) showed that associated bacteria can supply the bloom-forming cyanobacterium *Raphidiopsis raciborskii* with nitrogen sources and hence regulate its growth and toxicity. Therefore, deciphering the interactions between heterotrophic bacteria and harmful algae is vital for understanding microbe-driven aquatic ecosystem processes and functions, including mass bloom development and toxicity (Dziallas and Grossart, 2012).

In bacterial communities, dominant (or common) and rare species often exhibit distinct distribution patterns and functional traits and are therefore expected to respond differently to variations in phytoplankton community composition and abundance (Liu et al., 2015; Wan et al., 2021). In previous studies, abundant taxa have been widely explored, while rare taxa remain largely unexamined (Liu et al., 2019; Nyirabuhoro et al., 2020). For example, microcystin degraders, Alphaproteobacteria of the family Sphingomonadaceae (*mlrA* genotype), respond to and affect the dynamics of toxic *Microcystis* blooms in various inland waters (Dziallas and Grossart, 2012; Lezcano et al., 2017; Zhu et al., 2014). *Rhizobium* sp. isolated from cyanobacterial bloom samples was found to promote the growth of *Microcystis aeruginosa* and enhance its resistance to H_2O_2 in co-cultures (Kim et al., 2021). *Phenylobacterium* interacted with toxic *Microcystis* and maintained its competitiveness against non-toxic *Microcystis* in Lake Taihu (Zuo et al., 2021). Yet, our understanding of rare taxa (alternatively known as "rare biosphere") (Sogin et al., 2006) and their ecological roles and functions in the aquatic system is still very sparse, in part because of methodological limitations. This is unfortunate as rare taxa are tremendously diverse and hold a disproportionate functional potential in the ecosystem (Dee et al., 2019; Jousset et al., 2017; Shade et al., 2014), an example being sulphate reduction in peatland ecosystems, which can be conducted by a single bacterial genus comprising $< 0.006\%$ of the whole microbial community (Pester et al., 2010) or by consortia of low-abundance bacteria (Hausmann et al., 2016).

Recently, advances in molecular approaches, single-cell detection techniques have substantially boosted our knowledge of the rare bacterial community (Dee et al., 2019; Jia et al., 2018; Jousset et al., 2017; Nyirabuhoro et al., 2020). In aquatic ecosystems, studies on rare taxa have mainly focused on their geographical distribution patterns, community assembly processes and the environmental driving factors (Liu et al., 2015; Mo et al., 2018; Nyirabuhoro et al., 2020). The biogeography of abundant and rare bacteria might follow similar spatial and temporal patterns (Wang et al., 2020), but their subcommunity assembly mechanisms can differ as in human-made cascade reservoirs of a large river (Chen et al., 2020). Furthermore, an extensive investigation in Chinese inland freshwaters revealed that rare bacterial taxa seemed limited more by local environmental conditions than by abundant species (Liu et al., 2015). In addition, the dispersal of rare bacterial taxa was more limited than that of abundant taxa in three subtropical Chinese bays (Mo et al., 2018). In contrast to abundant taxa, rare bacteria exhibited stronger environmental adaptation in response to dredging in eutrophic Lake Nanhu (Wan et al., 2021), indicating substantial differences in community behaviour between rare and abundant bacterial taxa. Co-occurrence network analysis also revealed that most keystone species were also rare (Chen et al., 2020; Wang et al., 2020), indicating that they play important roles in community structure and assembly processes (Bickel and Or, 2021; Jousset et al., 2017) as well as ecosystem functions (Pester et al., 2010). However, many functions of rare bacteria in aquatic ecosystems, including reservoirs, are not well studied. In particular, the current findings on species interactions based solely on field investigations without any solid causal relationship back-up are not sufficient to reveal the ecological roles of rare bacteria and the mechanisms involved. Recent studies have highlighted the need for integrating associated analyses with culture experiments in order to demonstrate the causality of bacterial interactions, e.g. in studies of gut microbiota (Zhao and Zhao, 2021), and such integration is also urgently needed in studies on microbial interactions related to rare bacteria in aquatic systems (Pound et al., 2021).

Raphidiopsis raciborskii is regarded as an emerging bloom-forming invasive cyanobacteria species in subtropical and temperate regions, and it is now distributed worldwide, especially in tropical/subtropical lakes and reservoirs (Antunes et al., 2015; Sidelev et al., 2020; Tan et al., 2021). Some strains of *R. raciborskii* can produce cylindrospermopsin (CYN) or paralytic shellfish poisoning (PSP) toxins, and these are of increasing ecological, environmental and economical concern due to their bioaccumulation and multi-organ toxicity (Scarlett et al., 2020; Yang et al., 2021). In China, this species can nowadays be found in many lakes and reservoirs (Lu et al., 2021; Yang et al., 2021), and it forms the second most toxic blooms after *Microcystis,* thereby greatly threatening human and aquatic ecosystem health. The increasing frequency, spatial expansion and toxicity of *R. raciborskii* blooms call for information on the mechanisms behind its formation and disappearance. There is a long history of studying the cyanobacteria-bacteria community interactions; yet, previous studies have largely focused on abundant or common bacterial species. Plankton communities are normally comprised of only a few abundant but many rare species; yet little is known about the ecological role of these rare bacterial species (Vico et al., 2021; Xue et al., 2018), even though these bacteria have the potential to interact and hence control the outbreak and expansion of *R. raciborskii* blooms. More knowledge of the role of rare bacteria is required, particularly concerning early-warming and prediction of *R. raciborskii* blooms, as well as regarding the management of blooms for water security.

In this 3-week study, different communities of rare bacteria were generated randomly by dilution-to-extinction and co-cultured with an *R. raciborskii* XM1 strain in the lab. This allowed us to study the interactions between the cyanobacterium and associated rare bacteria by measuring cyanobacterial photosynthesis via Phyto-PAM and bacterial community composition via 16S rRNA gene amplicon sequencing. Owing to differences in cell abundance, extremely rare bacterial species will disappear first with increasing dilution, hence a majority of rare species are either absent or present, and species coexistence relationships between rare taxa will be broken, while abundant bacterial species are less abundant, but always present, and may potentially develop higher densities. Therefore, we proposed three hypotheses: (i) a dilution threshold for rare species exists, above or below which they have differential effects on the bloom-forming cyanobacterium *R. raciborskii*; (ii) rare bacterial species influence *R. raciborskii* photosynthesis and growth through specific interactions; (iii) network-coexistent relationships can be used to identify specific rare species that interact closely with *R. raciborskii* and regulate important ecosystem functions.

2. Materials and methods

2.1. *Raphidiopsis raciborskii* cultures and microorganisms in different reservoirs

R. raciborskii XM1 was isolated from Shidou Reservoir in Xiamen, China, in 2018 (Tan et al., 2021). The cultures of *R. raciborskii* XM1 were maintained in BG-11 medium (Rippka et al., 1979) under a constant and cool fluorescent light with an intensity of 30 ± 2 μmol photons/(m^2·s) using a light and darkness cycle of 12 h at 28 °C and 12 h at 26 °C, respectively. Before inoculation, all *R. raciborskii* XM1 cells were cultured for 30–40 days in acid-washed, cotton-plugged sterile flasks to reach the exponential growth stage (Fig. S1).

To obtain the inocula, surface water samples were taken at 0.5 m depth in different reservoirs (Shidou, Bantou, Tingxi and Xinglinwan) in Xiamen city. Twelve litres of water were sampled from Shidou Reservoir on 20 October and 28 November 2020 for two different batches of the experiment. Meanwhile, 1 L water was separately taken from Tingxi Reservoir, Bantou Reservoir and Xinglinwan Reservoir on 22 October,

28 November and 1 December 2020. To generate the sterilised water to be used in the experiments, 11 L of water were collected from Shidou Reservoir and filtered through glass microfiber filters (0.7 μm pore size, 47 mm diameter, Whatman GF/F, GE Healthcare Life Sciences, Buckinghamshire, UK) and subsequently through 0.22 μm pore size filter membranes (47 mm diameter, Isopore, Merck Millipore, Tullagreen, Carrigtwohill, Ireland) to eliminate microorganisms. Next, all filtrates were autoclaved for the subsequent experiments. A 1 L of water sample from each reservoir was kept at room temperature until the start of the experiments.

2.2. Experimental setup

To obtain rare bacterial species and test their interactions with the invasive cyanobacterium *R. raciborskii* XM1, we manipulated the density of bacterial species using a dilution-to-extinction approach and co-cultured the bacteria with *R. raciborskii* XM1. We maintained equal amounts of whole bacteria in the same orders of magnitude in all treatments before dilution and regulated the relative abundance of bacteria by a diluting approach. The relative abundance of the most abundant bacterial species decreased, while many rare bacterial species disappeared. Two batch experiments were run successively (Fig. 1).

In experiment A, we hypothesised that 10,000-fold dilution would be a key dilution level for rare bacterial species. Shidou Reservoir original water was diluted with sterilised Shidou Reservoir water to generate four dilutions between 10^{-3} and 10^{-6} (D_{3A}, D_{4A}, D_{5A}, D_{6A} treatments, Fig. 1). At the same time, original water from Tingxi Reservoir (a reservoir located not far away from Shidou Reservoir whose bacterial community has a low similarity to Shidou Reservoir) was also diluted to 10^{-4} with sterilised Shidou Reservoir water and served as a control (D_{TX}

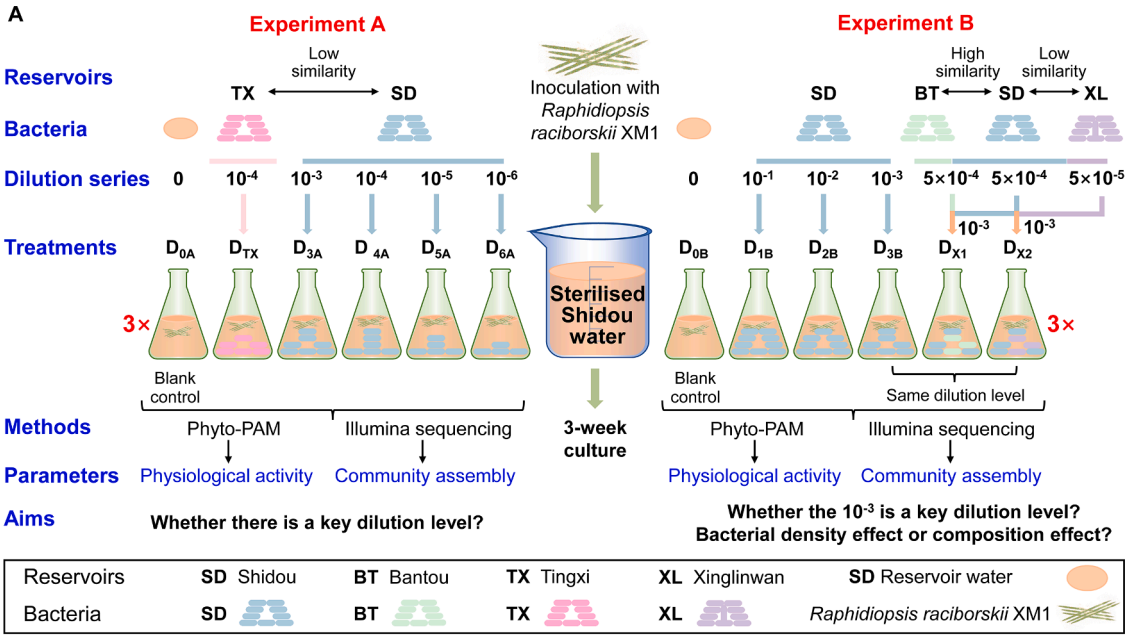

B

222 samples = 33 field samples + 9 BG11 samples + 36 D_{3L} samples + 144 treatment samples

Experiment setup			Sampling day																Sequencing
Batch	Dilution	Treatment	0	1	3	5	6	7	8	10	12	13	14	15	17	20	21	22	32	Number
Experiment A	0	BG11						*					*						*	9 (3 × 3)
	0	D_{0A}	**	*	*	*		**		*	*		**				*			12 (4 × 3)
	10^{-3}	D_{3A}	**	*	*	*		**		*	*		**				*			12 (4 × 3)
	10^{-4}	D_{4A}	**	*	*	*		**		*	*		**				*			12 (4 × 3)
	10^{-5}	D_{5A}	**	*	*	*		**		*	*		**				*			12 (4 × 3)
	10^{-6}	D_{6A}	**	*	*	*		**		*	*		**				*			12 (4 × 3)
	10^{-4}	D_{TX}	**	*	*	*		**		*	*		**				*			12 (4 × 3)
Experiment B	0	D_{0B}	**	*	*		*	*	*	*		*	*	*	*	*	*	*		12 (4 × 3)
	10^{-1}	D_{1B}	**	*	*		*	*	*	*		*	*	*	*	*	*	*		12 (4 × 3)
	10^{-2}	D_{2B}	**	*	*		*	*	*	*		*	*	*	*	*	*	*		12 (4 × 3)
	10^{-3}	D_{3B}	**	*	*		*	*	*	*		*	*	*	*	*	*	*		12 (4 × 3)
	10^{-3}	D_{X1}	**	*	*		*	*	*	*		*	*	*	*	*	*	*		12 (4 × 3)
	10^{-3}	D_{X2}	**	*	*		*	*	*	*		*	*	*	*	*	*	*		12 (4 × 3)
	10^{-3}	D_{3L}	**	*	*	*	*		*	**		**		*	**	*		**		36 (6 × 6)

* Phyto-PAM * Sequencing

Low dilution High dilution

Fig. 1. Overview of experimental design. (A) Experimental procedures and (B) sampling schemes. Sterilised Shidou water was used as bulk water to dilute raw water from the Shidou, Tingxi, Bantou and Xinglingwan reservoirs and thus produce a series of different densities and compositions of microorganisms. In experiment A, we hypothesised that 10^{-4} dilution is a key dilution level, which significantly influences the interactions between rare bacterial species and *Raphidiopsis raciborskii* XM1. Besides the negative control, Tingxi water with 10^{-4} dilution also served as control. Using the results of experiment A, experiment B was run immediately after. Treatments with 10^{-1} and 10^{-2} dilution were amended. At the same time, to eliminate bacterial density or community composition effects, two mixed dilutions (half Bantou or Xinglinwan water plus half Shidou water to obtain a mixed dilution of 10^{-3}) were created. All treatments were inoculated with *R. raciborskii* XM1 and cultured for 22 days. Phyto-PAM and Illumina sequencing approaches were used to measure the changes in the physiology of *R. raciborskii* XM1 and bacterial community composition, respectively.

treatment). Untreated sterilised Shidou Reservoir water served as negative control (D_{0A} treatment).

Experiment A suggested that 1000-fold dilutions inhibited the growth of *R. raciborskii* XM1, but was that also the case for the < 1000-fold dilution? To elucidate this, experiment B was carried out to answer the following two questions: (1) Is the ≤1000-fold dilution a threshold dilution level that may significantly inhibit the growth of *R. raciborskii* XM1, (2) Do changes in bacterial density and/or community composition influence the growth of *R. raciborskii* XM1 (Fig. 1)? In experiment B, we had three dilution levels, ranging from 10^{-1} to 10^{-3}(D_{1B}, D_{2B} and D_{3B} treatments), two mixed treatments (D_{X1}, D_{X2} treatments) and one negative control (D_{0B} treatment) (Fig. 1A). Based on historical data of 16S rRNA gene copy numbers by qPCR (Mo et al., 2021), 5×10^{-4} dilutions of Bantou Reservoir original water and 5×10^{-5} dilutions of Xinglinwan Reservoir original water were separately mixed with 5×10^{-4} dilutions of Shidou water to obtain the two mixed dilutions with 10^{-3} (D_{X1} and D_{X2} treatments). Shidou, Bantou and Xinglinwan reservoirs are all located in Houxi watershed, but as Bantou Reservoir is located next to Shidou Reservoir, the bacterial community similarity is likely higher between Shidou and Bantou reservoirs than between Shidou and Xinglinwan reservoirs. Therefore, the D_{3B}, D_{X1} and D_{X2} treatments in experiment B had the same dilution level with different community compositions (Fig. 1A).

All treatments with the same total volumes were inoculated with the same amounts of *R. raciborskii* MX1 (inocula in triplicate) and were maintained in clean, acid-washed Erlenmeyer flasks (180 mL cultures in 250 mL) for about 22 days.

In both experiment A and experiment B, 3 mL subsamples were collected on specific days (Fig. 1B). One microlitre was used to monitor the growth of *R. raciborskii* XM1 via absorbence at 680 nm, and 2 mL were applied to measure photosynthetic parameters using a Phyto-PAM Phytoplankton analyser (Heinz Walz GmbH, Effeltrich, Germany). At the beginning of the experiment, 100 mL subsamples were collected for DNA extraction, and 40 mL subsamples were collected on days 0, 7, 14 and 21. These subsamples were filtered onto 0.22 μm pore-size polycarbonate filters (47 mm diameter, Isopore, Merck Millipore, Tullagreen, Carrigtwohill, Ireland) for genomic DNA sequencing to determine microbial community composition. The filters were stored at –80 °C until further processing in the lab.

We collected four subsamples to determine microbial community composition during the growth period of the *R. raciborskii* XM1 culture with inocula of the different bacterial dilutions. To track changes or shifts in microbial community compositions during cultivation, dilutions to 10^{-3} were repeatedly run in a larger culture setup (360 mL cultures in 500 mL-flask, D_{3L} treatment) in experiment B. On days 0, 5, 10, 13, 17 and 22, 35–40 mL subsamples were collected to determine the microbial community composition. In addition, subsamples from BG11 medium cultures of *R. raciborskii* XM1 (BG11 treatment) were collected on days 7, 14 and 32 to identify bacteria directly associated with *R. raciborskii* XM1.

2.3. Lab-cultured and field-collected samples

In total, we had 189 lab culture samples, including 144 treatment samples (12 treatments × 3 replicates × 4 sampling times), 9 BG11 treatment samples and 36 D_{3L} treatment samples (6 replicates × 6 sampling times) (Fig. 1B). To assess the community differences between the cultured samples and natural communities, 24 field samples were also included in our study. Based on previous information (Tan et al., 2021), two high and two low *R. raciborskii* abundance periods based on both microscope-based cell numbers and PCR-based gene copy numbers were selected for sampling in Shidou and Bantou reservoirs at three sites in each. Before setting-up experiments A and B, original bacterial communities were collected from raw reservoir water (9 samples, 3 and 6 samples were taken on 20 October and 28 November in 2020, respectively), and we thus had a total of 33 undiluted field samples (Fig. 1B).

2.4. Comparison of different dilution groups

We had two negative controls (D_{0A} treatment in experiment A and D_{0B} treatment in experiment B) and two mixed controls (D_{X1} and D_{X2} treatments). Based on the dilution level, the D_{1B}, D_{2B}, D_{3A}, D_{3B} and D_{3L} treatments acted as low-dilution groups and the D_{4A}, D_{5A}, D_{6A} and D_{TX} treatments as high-dilution groups. However, the results of the D_{X1} and D_{X2} treatments were similar to those of the low-dilution groups because, although the community compositions of D_{3B}, D_{X1} and D_{X2} treatments differed, they still had relatively high similarities. The D_{0A}, D_{0B} and BG11 treatment results were similar to those of the high-dilution groups because the negative control represents infinite dilution. Hence, for simplification and visualisation, 222 samples were separated into three groups, including undiluted (field samples, $n = 33$), low-dilution (D_{1B}, D_{2B}, D_{3A}, D_{3B}, D_{X1}, D_{X2} and D_{3L} treatments, $n = 108$) and high-dilution groups (D_{0A}, D_{0B}, D_{4A}, D_{5A}, D_{6A}, D_{TX} and BG11 treatments, $n = 81$). When culture time was included in the analysis, BG11, the D_{3L} treatments and undiluted samples were excluded. Therefore, only 144 samples were considered in the analysis of temporal changes, including the low-dilution (D_{1B}, D_{2B}, D_{3A}, D_{3B}, D_{X1} and D_{X2} treatments) and high-dilution groups (D_{0A}, D_{0B}, D_{4A}, D_{5A}, D_{6A} and D_{TX} treatments) ($n = 18$, for each sampling day in all groups).

For comparing the difference in the treatments, we calculated the growth inhibition rate by the formula:

$$rate_x = 100 - \frac{C_{treatment}}{C_{control}} \times 100\%$$

where x means the culture time (day 10, day 14 or day 15), $C_{treatment}$ means the Chl-*a* concentration in the different treatments on day x, and $C_{control}$ means the Chl-*a* concentration in the control D_{0A} or D_{0B} on day x in experiments A and B, correspondingly.

2.5. Photosynthetic parameters

Photosynthetic activities of the culture samples were measured by a Phytoplankton analyser, Phyto-PAM (—PHYTO-C, Phyto-PAM-ED, Heinz Walz GmbH, Effeltrich, Germany). Rapid light curves, plotted by the relative electron transfer rate (ETR) versus irradiance (I) curves at different photosynthetic available radiation (PAR) levels, provide detailed information on the saturation characteristics of electron transport and on the overall photosynthetic performance of a plant (Ralph and Gademann, 2005). Measurements of Fv/Fm (maximum quantum efficiency of photosystem II), Yield (photosystem II operating efficiency), Chl-*a*, α (efficiency of electron transport), ETR_{max} (maximum ETR) and I_k (half-saturating light intensity for the photosynthesis) (Kalaji et al., 2014; Perri et al., 2021) were performed in the dark. Two-millilitre subsamples of the culture were transferred to a 5 mL glass tubes, stirred and dark adapted at room temperature for at least 5 min (5–8 min). After dark adaption, measurements were performed step-by-step according to the manufactory's protocol. The "blue" algae reference spectrum file for the Phyto-PAM was obtained using the manufacturer's protocol from a culture of *R. raciborskii* XM1, and "green" and "brown" algae reference spectrum files were acquired using *Chlorella vulgaris* FACHB 38 and *Cyclotella meneghiniana* FACHB 2822, which are the most common and abundant *Chlorophyta* and *Bacillariophyta* in reservoirs of the Fujian Province, China (Lv et al., 2014). These two strains were provided by the Freshwater Algae Culture Collection at the Institute of Hydrobiology, Chinese Academy of Sciences (Wuhan, China).

To monitor the growth of the *R. raciborskii* XM1 culture, OD_{680} was measured by a UV-visible spectrophotometer (TU-1810, Beijing Purkinje General Instrument, Beijing, China). A 1-millilitre subsample was put into a micro and 1-cm quartz cuvette, after which absorbence values for

the sample were recorded at a wavelength of 680 nm.

2.6. Characterisation of the microbial community

During the experiments, microbial community compositions were characterised using 16S rRNA gene amplicon sequencing. Microbial DNA was extracted from the 0.22 μm pore size membrane for each subsample using FastDNA Spin Kit (MP Biomedicals, Solon, OH, USA). The 16S rRNA gene of V3-V4 regions was amplified using the specific primer set 341F (5′-CCTAYGGGRBGCASCAG-3′) and 806R (5′-GGACTACNVGGGTWTCTAAT-3′) with barcodes and sequenced using the Illumina NovaSeq platform (Illumina, Inc., San Diego, CA, USA) through a paired-end (2 × 250 bp) sequencing strategy. All PCR reactions were performed in 20 μL volumes in triplicate and included 10 μL Takara Premix Taq (Ex Taq version 2.0 plus dye, Takara Bio, Kusatsu, Shiga, Japan), 0.25 μM of each primer and 10 ng microbial DNA. The qPCR program was initiated with a 5-min hold at 95 °C, followed by 30 cycles that included a denaturing step at 95 °C for 30 s, an annealing step at 55 °C for 30 s, an elongation step at 72 °C for 30 s and a final extension at 72 °C for 5 min. The PCR products from triplicate reactions per sample were pooled for gel purification and sequencing.

2.7. Bioinformatics

Paired-end reads from the amplicon sequencing data were processed using VSEARCH v.2.14.1 (Rognes et al., 2016). After merging the paired-end reads by MOTHUR v1.39.5 (Schloss et al., 2009) to get raw reads, quality filtering of the raw reads was performed using the "minuniquesize 8″ parameter in VSEARCH for generating unique sequences. Unoise3 algorithm was used to discard chimeras and assign zero-radius operational taxonomic units (Zotus) at a 97% sequence similarity threshold in USEARCH v11 (Edgar, 2010, 2016). A representative sequence for each Zotu was screened for further annotation. All representative sequences were taxonomically classified by USEARCH v11 against the SILVA rRNA gene database (release 138.1) (Quast et al., 2013). All archaea, chloroplasts, mitochondria, eukaryota and unknown sequences were discarded. Finally, the whole Zotu dataset was randomly normalised to 61,452 sequences, and all sequences were clustered into 3664 Zotus.

2.8. Definition of abundant and rare taxa

The cutoffs for defining abundant and rare taxa are arbitrary, so there is no fixed golden threshold for differentiating between abundant and rare species (Jia et al., 2018). In this study, we classified all Zotus into six categories following our previous studies (Chen et al., 2019; Nyirabuhoro et al., 2020; Xue et al., 2018): (i) always abundant taxa (AAT), Zotus with a relative abundance $\geq$ 1% in all samples; (ii) conditionally abundant taxa (CAT), Zotus with a relative abundance $\geq$ 1% in some samples and $\geq$ 0.01% in other samples, but never $<$ 0.01%; (iii) conditionally abundant or rare taxa (CRAT), Zotus with a relative abundance from rare $<$ 0.01% to abundant $\geq$ 1% in all samples; (iv) moderate taxa (MT), Zotus with a relative abundance $<$ 1% and $\geq$ 0.01% in all samples; (v) conditionally rare taxa (CRT), Zotus with $<$ 0.01% local relative abundance in some samples and $\geq$ 0.01% in others, but never $\geq$ 1%; (vi) always rare taxa (ART), Zotus with relative abundance $<$ 0.01% in all samples.

2.9. Network construction

Molecular ecological network analysis (MENA) networks were constructed using the MENA pipeline on the basis of Pearson correlations of log-transformed Zotu abundances, followed by a random matrix theory-(RMT-) based approach (Zhou et al., 2010), which automatically determines the correlation cut-off threshold for network construction (http://ieg4.rccc.ou.edu/MENA/) (Deng et al., 2012). Each network was constructed independently by applying a unique set of biological samples, and only Zotus present in more than half of all samples were included for correlation calculation. The Pearson correlation coefficient was calculated for each pair of Zotus on the basis of the Zotus' log-transformed relative abundances. The raw correlation matrix was analysed with the RMT-based network approach, the first cutoff value was subsequently chosen as the cutoff threshold when $P \geq 0.05$ in a Chi-square test. An adjacency matrix was generated, including only the correlations with absolute coefficient values $\geq$ the threshold. Nodes in an adjacency matrix without a correlation coefficient with other nodes were removed from the network. After that, an undirected network graph was drawn.

Nodes (total nodes or Zotus), links (total links or significant correlations), density, modularity, average K (average degree), average CC (average clustering coefficient), average PD (average path distance), connectedness and other topological properties were all directly generated by the MENA pipeline. The constructed networks were visualised using Cytoscape (version 3.8.2) and Gephi (version 0.9.2) with an adjacency matrix generated by greedy modularity optimisation to run module separation in the pipeline. Small-W (small-world coefficient) was calculated with the "igraph" packages in R software (version 4.0.3). Small-W was calculated by the formula: $(C/C_{random})/(L/L_{random})$, where C is the empirical network average CC, and C_{random} is the random network average CC, while L is the empirical network average PD, and L_{random} is the random network average PD. Robustness was measured as the proportion of taxa remaining when 50% of the taxa were randomly removed from each of the empirical MENA networks with 100 repetitions of the simulation. Stability (bacterial community compositional stability) of the network community over time is based on composition differences between every two adjacent samplings. Robustness, vulnerability and compositional stability were all calculated in R software with the code referenced by Yuan et al. (2021). Following the definition of Olesen et al. (2007), keystone nodes were detected on the basis of their within-module connectivity (*Zi*) and among-module connectivity (*Pi*).

2.10. Statistical analyses

Bacterial community composition was visualised by non-metric multidimensional scaling (NMDS) with square root transformation and Wisconsin double standardisation in the "vegan" package using R software (version 4.0.3). Analysis of similarities (ANOSIM) was used to test for significant differences between groups. Shared OTU numbers between the samples from two continuous samplings were visualised by a Sankey diagram and plotted with the "networkD3" and "d3Network" R packages. The species diversity index was calculated for each sample using the diversity function in the "vegan" package, while phylogenetics diversity index was computed by the function in the "picante" package. Niche width and overlap were calculated in the "spaa" package. Analysis of Wilcoxon rank sum tests was used to examine differences between different groups or among groups between different days.

A neutral community model (NCM) predicting the relationship between the detection frequency and relative abundance of OTUs across the whole metacommunity was used to determine the potential importance of stochastic processes for the community assembly (Sloan et al., 2006). *Nm* is an estimate of dispersal between communities, which determines the correlation between occurrence frequency and relative abundance, with *N* describing the metacommunity size and *m* presenting the immigration rate. The parameter R^2 shows the overall fit with the neutral model. Calculation of 95% confidence intervals around all fitting statistics was done by bootstrapping with 1000 bootstrap replicates with previous R codes (Chen et al., 2019).

3. Results

3.1. Growth and photosynthetic activity of Raphidiopsis raciborskii XM1

Under high nitrogen and phosphorus conditions (BG11 medium), *R. raciborskii* XM1 grew fast with a generation time of 2.5 days and reached the stationary phase after 40 days (Fig. S1). Under ambient nutrient conditions (reservoir water, low nitrogen and phosphorus), the cyanobacterial growth was also relatively high during the first few days of both experiment A and experiment B, but the treatments showed significantly different growth responses with increasing incubation time (Fig. 2).

In experiment A, the growth of *R. raciborskii* XM1 increased during the first days but decreased on day 5 for the D_{3A} treatment, while it increased until the end of the experiment for the D_{0A} (negative control), D_{TX}, D_{4A}, D_{5A} and D_{6A} treatments (Fig. 2A). Variations in photosynthetic activity showed that only the D_{3A} treatment exhibited significant differences in photosynthetic activity throughout the whole experiment A, while all other treatments and the negative control did not change notably (Fig. S2A). In experiment B, the growth of *R. raciborskii* XM1 in the D_{1B}, D_{2B}, D_{3B} and D_{X1} treatments was similar to the D_{3A} treatment in experiment A, while in the D_{0B} treatment (negative control) it was similar to the D_{0A} treatment in experiment A (Fig. 2B). In the D_{X2} treatment, *R. raciborskii* XM1 growth was inhibited but to a lesser extent than in the other treatments showing growth inhibition (Fig. 2B, Table 1). That is, variations in photosynthetic activity in the D_{2B}, D_{3B} and D_{X1} treatments exhibited differences on day 8, whereas the photosynthetic activities of *R. raciborskii* XM1 rapidly dropped on day 13 in the D_{X2} treatment (Fig. 2B). In the later culture period of experiment B, *R. raciborskii* XM1 growth was also inhibited because of nutrient limitation.

Taking into consideration the physiology of *R. raciborskii* in experiments A and B, 1000-fold dilution represented a threshold dilution level, i.e. the growth of *R. raciborskii* XM1 was significantly inhibited at this or lower dilution levels.

3.2. Changes in bacterial community composition, diversity and niche width

It is evident that the dilution approach had significant impacts on the bacterial community composition (Fig. 3). Nonmetric multidimensional scaling (NMDS) analysis based on Bray-Curtis dissimilarity showed that the dilution groups could be distinguished from each other, especially the undiluted group (field-collected samples), which differed greatly from the lab cultures, including both the low-dilution groups (D_{1B}, D_{2B}, D_{3A}, D_{3B}, D_{X1}, D_{X2} and D_{3L} treatments) and the high-dilution groups (D_{0A}, D_{0B}, D_{4A}, D_{5A}, D_{6A}, D_{TX} and BG11 treatments) (Fig. 3A, global $R_{Group} = 0.612$, $P < 0.01$). To evaluate the changes in bacterial community compositions over time, field samples and the D_{3L} and BG11 treatments were excluded and reanalysed with NMDS. The results showed that there were significant differences between groups (between the low-dilution groups and the high-dilution groups, global $R_{Group} = 0.358$, $P < 0.01$) and between treatments (between all treatments, global $R_{Treatment} = 0.345$, $P < 0.01$), but no significant differences within groups (neither within the low-dilution groups nor the high-dilution groups). The low-dilution groups (D_{1B}, D_{2B}, D_{3A}, D_{3B}, D_{X1} and D_{X2} treatments) deviated increasingly over time, while the high-dilution groups (D_{0A}, D_{0B}, D_{4A}, D_{5A}, D_{6A} and D_{TX} treatments) diverged into an opposite direction (global $R_{Day} = 0.270$, $P < 0.01$), indicating that the low- and high-dilution groups developed in an increasingly different direction over time (Fig. 3B).

Dilution influenced the initial bacterial community compositions, and high-dilution led to greater loss of the α-diversity of bacterial communities (Fig. S3). All species diversity indices, including Zotu number, Shannon-Wiener index, Simpson index and Pielou's evenness index, significantly ($P < 0.01$) decreased with increasing dilution (Fig. S3A-D). The phylogenetic diversity indices were different from the species diversity indices. The net relatedness index and the nearest taxon index were significantly lower in the low-dilution groups than in the high-dilution groups (Fig. S3E-F).

The niche widths of the bacterial communities were also influenced by dilution, and the width significantly increased in the higher dilution treatments (Fig. S4A). Niche overlaps of treatments in the undiluted and low-dilution groups were similar but significantly lower than in the

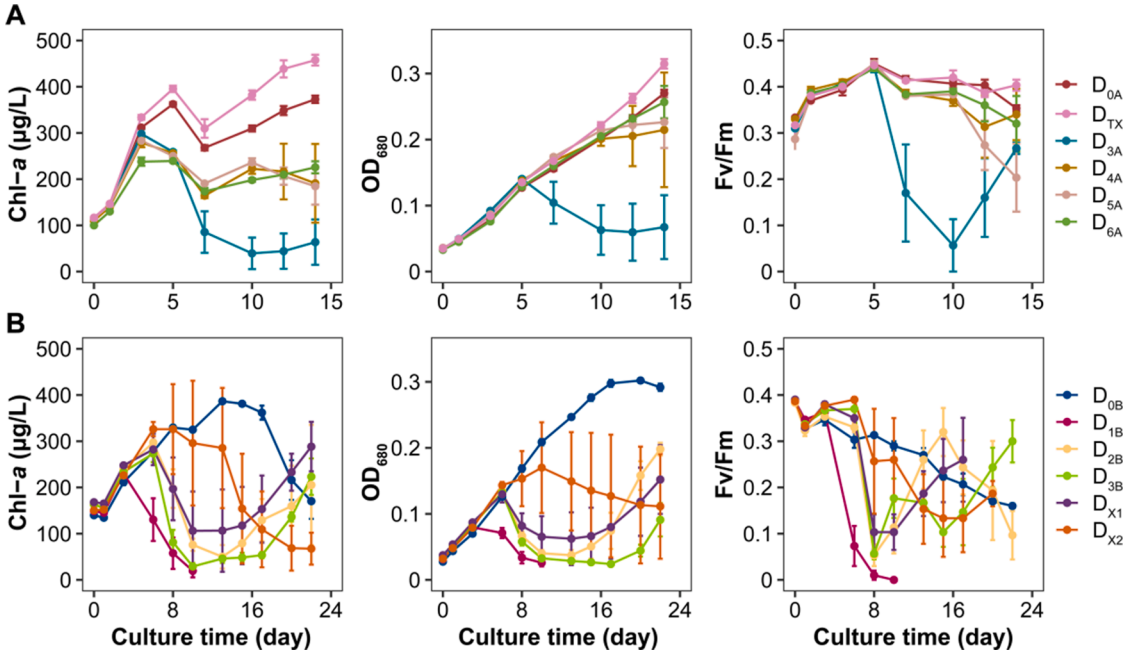

Fig. 2. Variations of physiological activities of *Raphidiopsis raciborskii* XM1 in experiments A and B over time. Variations of Chl-*a*, OD_{680} and Fv/Fm in experiments A (A) and B (B) were evaluated separately. Data are mean ± SE ($n = 3$).

Table 1
Growth inhibition rate of the different treatments in experiments A and B.

Treatment	Day 10 Chl-*a* (μg/L)	Rate (%)	Day 14 Chl-*a* (μg/L)	Rate (%)	Treatment	Day 10 Chl-*a* (μg/L)	Rate (%)	Day 15 Chl-*a* (μg/L)	Rate (%)
D_{0A}	309.68	0	372.87	0	D_{0B}	324.95	0	381.06	0
D_{TX}	382.01	-23.36	457.59	-22.72	D_{1B}	19.53	93.99	ND	ND
D_{3A}	39.46	87.26	63.70	82.92	D_{2B}	75.89	76.65	79.15	79.23
D_{4A}	222.53	28.14	191.02	48.77	D_{3B}	29.07	91.06	48.32	87.32
D_{5A}	236.20	23.73	184.74	50.45	D_{X1}	106.13	67.34	117.56	69.15
D_{6A}	198.06	36.04	225.71	39.47	D_{X2}	295.94	8.93	154.20	59.53

Note that negative values mean promotion.
ND: not detected.

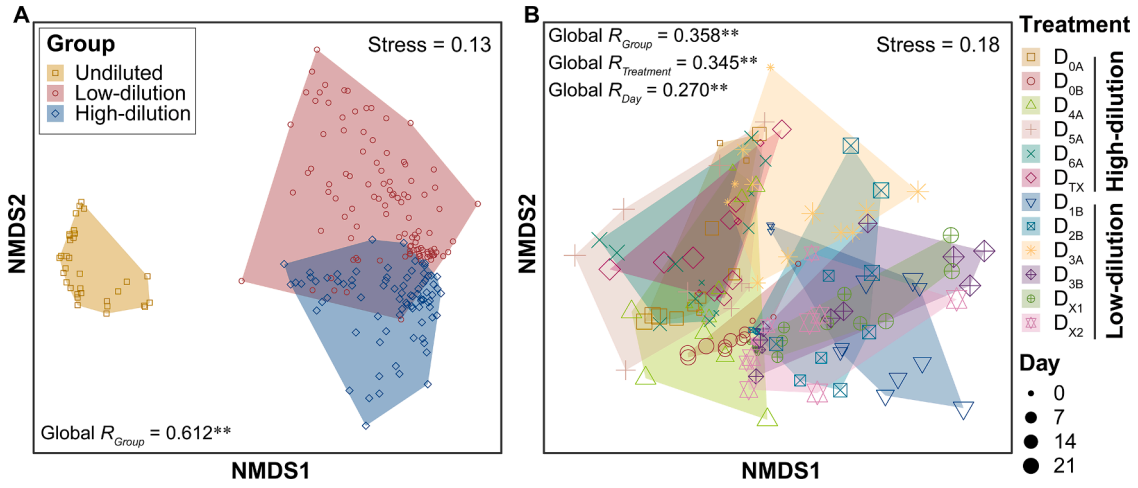

Fig. 3. Non-metric multidimensional scaling (NMDS) ordination showing the variation in the bacterial community. A: All samples including field and culture samples; B: lab culture samples (field samples, D_{3L} and BG11 treatments were excluded). Undiluted: field samples; low-dilution groups: D_{1B}, D_{2B}, D_{3A}, D_{3B}, D_{X1}, D_{X2} and D_{3L} treatments; high-dilution groups: D_{0A} (regarded as infinite dilution), D_{0B}, D_{4A}, D_{5A}, D_{6A}, D_{TX} and BG11 treatments. $^{**}P < 0.01$.

high-dilution groups (Fig. S4B). The niche width of bacterial communities in the high-dilution groups did not change significantly with time, but it decreased significantly in the low-dilution groups (Fig S4C). Moreover, except for day 0, the niche widths in the low-dilution groups were always lower than in the high-dilution groups, i.e. on days 7, 14 and 21 (Fig. S4C).

3.3. Bacterial dynamics and community assembly in response to *R. raciborskii* growth

To track the dynamics of different taxa categories (AAT: always abundant taxa; ART: always rare taxa; CAT: conditional abundant taxa; CRT: conditional rare taxa; CART: conditional abundant and rare taxa; MT: moderate taxa), all Zotu taxa at the previous sampling occasion ($n = 18$) in the low- or high-dilution groups were compared to those of the next sampling (i.e. day 0 to day 7, day 7 to day 14 or day 14 to day 21), which resulted in shared Zotu numbers for six taxa categories (Fig. 4). The majority of the Zotus belonged to ART and CRT. In the low-dilution groups, ART OTU number contribution gradually decreased over time, and CRT and CART gradually increased; while in the high-dilution groups, ART OTU number decreased over time, CART increased slightly, and CRT contribution did not change significantly (Fig. 4). Comparison of the low-dilution groups with the high-dilution groups, showed a rapid shift between rare taxa at low dilution.

With the growth of *R. raciborskii*, deterministic and stochastic processes in the bacterial community assembly conspicuously changed (Fig. S5). On day 0 (initial stage), the bacterial community assembly in the low- and high-dilution groups all matched the neutral community model ($R^2 = 0.76$ for low-dilution and 0.71 for high-dilution, respectively), reflecting the fact that the bacterial community assembly was strongly driven by stochastic processes. On day 7, the explained bacterial community variation in the low-dilution groups rapidly decreased from 76% to 54% and further to 40% at the end of the experiment (day 21). This reveals that deterministic processes became the main driver for the community assembly. However, in the high-dilution groups, the explained variation in community composition on day 7 did not vary notably (0.71 on day 0, 0.72 on day 7) and slightly decreased on days 14 (0.63) and 21 (0.58), suggesting that deterministic processes became stronger, but the stochastic processes still prevailed.

3.4. Shifts in topological properties of bacterial networks over time

To address the interactions in the different bacterial communities, eight time-series MENA networks (Fig. 5, Fig. S6) were constructed. The topological properties of bacterial empirical MENA networks exhibited distinct changes with cultivation time (Fig. 5, Table S1). Total nodes increased from day 0 to day 14 and slightly decreased on day 21, but in the low-dilution groups they were always higher than in the high-dilution groups (Fig. 5A). Total links, density, average K (average degree) and average CC (average clustering coefficient) all gradually decreased over time in all groups. Yet, in the low-dilution groups, this decline was more notable and had a higher coefficient of variation (Fig. 5B-C, Fig. 5E-F). This indicated that network coherence and complexity were much lower in the low-dilution groups. Generally, modularity increased (Fig. 5D), implying that environmental heterogeneity became stronger over time. The same pattern was observed for average PD (average path distance) (Fig. 5G). Moreover, over time, connectedness was substantially reduced in the low-dilution groups but increased gradually in the high-dilution groups (Fig. 5H). Altogether, these results suggest that dilution substantially alters the network

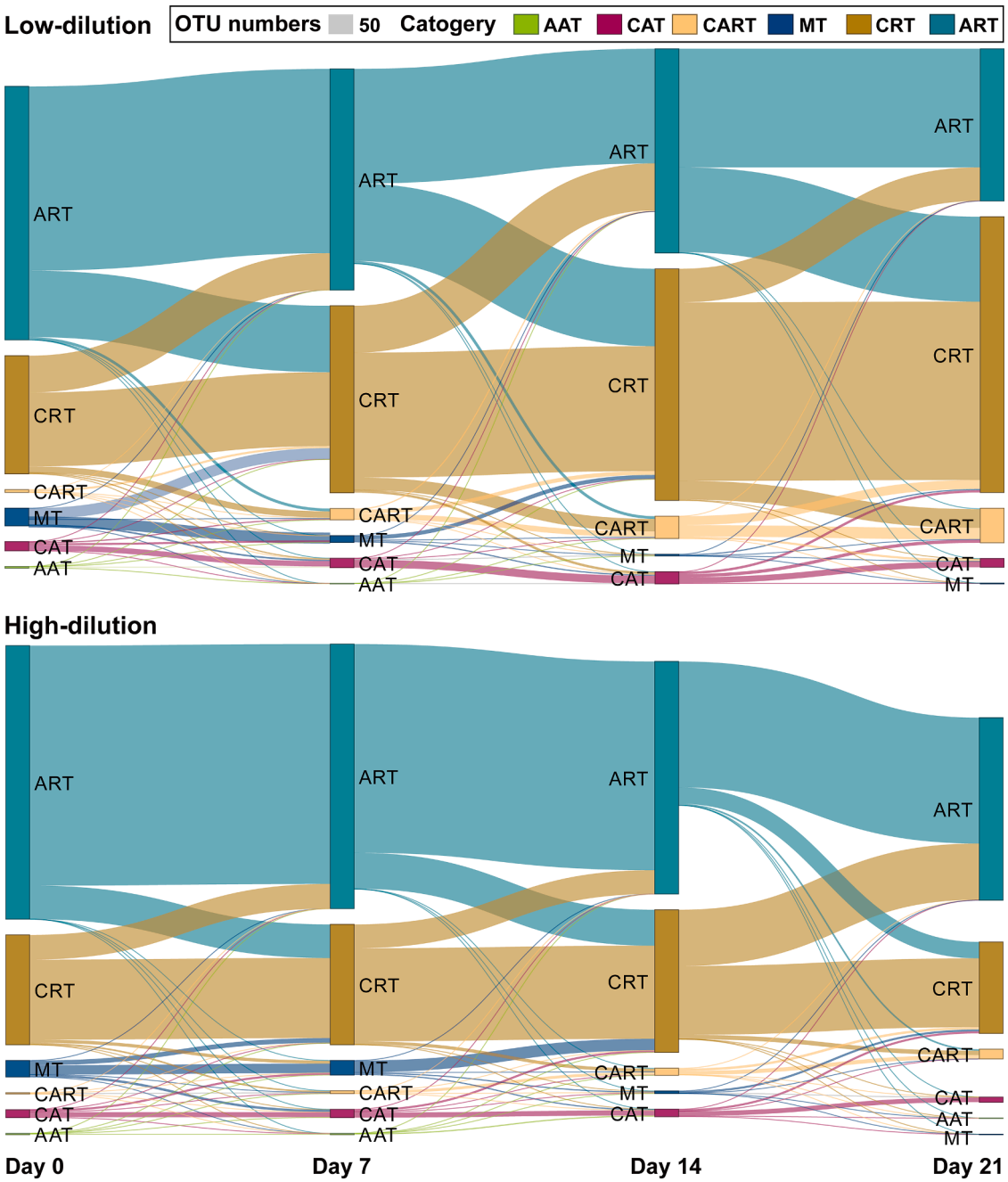

Fig. 4. Variation of the shared OTU numbers between the two continuous samplings. The low-dilution groups included the D_{1B}, D_{2B}, D_{3A}, D_{3B}, D_{X1} and D_{X2} treatments, and the high-dilution groups included the D_{0A} (regarded as infinite dilution), D_{0B}, D_{4A}, D_{5A}, D_{6A} and D_{TX} treatments. OTUs of each of the six categories in the former samples were compared to the six categories in the later samples, producing the shared OTU numbers as indicated by the height of the bar chart. AAT: always abundant taxa; ART: always rare taxa; CAT: conditional abundant taxa; CRT: conditional rare taxa; CART: conditional abundant and rare taxa; MT: moderate taxa.

topography at the higher-level organisation and that low-dilution groups have simpler hierarchical structures and harbour less closely associated microbial food webs.

The altered network structure and complexity indicate potential changes in the role of individual species within the MENA network. A total of 17 module hubs and six connectors were detected across the studied eight networks, consisting of Proteobacteria, Bacteroidetes, Cyanobacteria, Actinobacteria, Armatimonadetes, Planctomycetes and Verrucomicrobia, belonging to 13 genera (or families when unclassified at the genus level) (Fig. S7, Table S2). *Fluviimonas* and unclassified Rhizobiaceae occurred most frequently in all networks. The low-dilution groups had more keystone nodes (14 OTUs) than the high-dilution groups (9 OTUs). The most detected keystone nodes occurred on day 14 in both the low- and the high-dilution groups. To assess the keystone species difference between natural bacterial assemblages and lab cultures, four networks from all samples, undiluted (field-collected), low- and high-dilution (lab-cultured), were constructed and a total of 20 keystone nodes were detected, consisting of Bacteroidetes, Actinobacteria, Cyanobacteria, Proteobacteria and Verrucomicrobia belonging to 14 genera (or families when unclassified at the genus level) (Fig. S8, Table S3). The undiluted group had most keystone nodes. There were several identical keystone nodes (same OTU or taxonomy) between subnetworks (networks for different culture times in the low- and high-dilution groups, Fig. S7) and overall-networks (networks for all samples

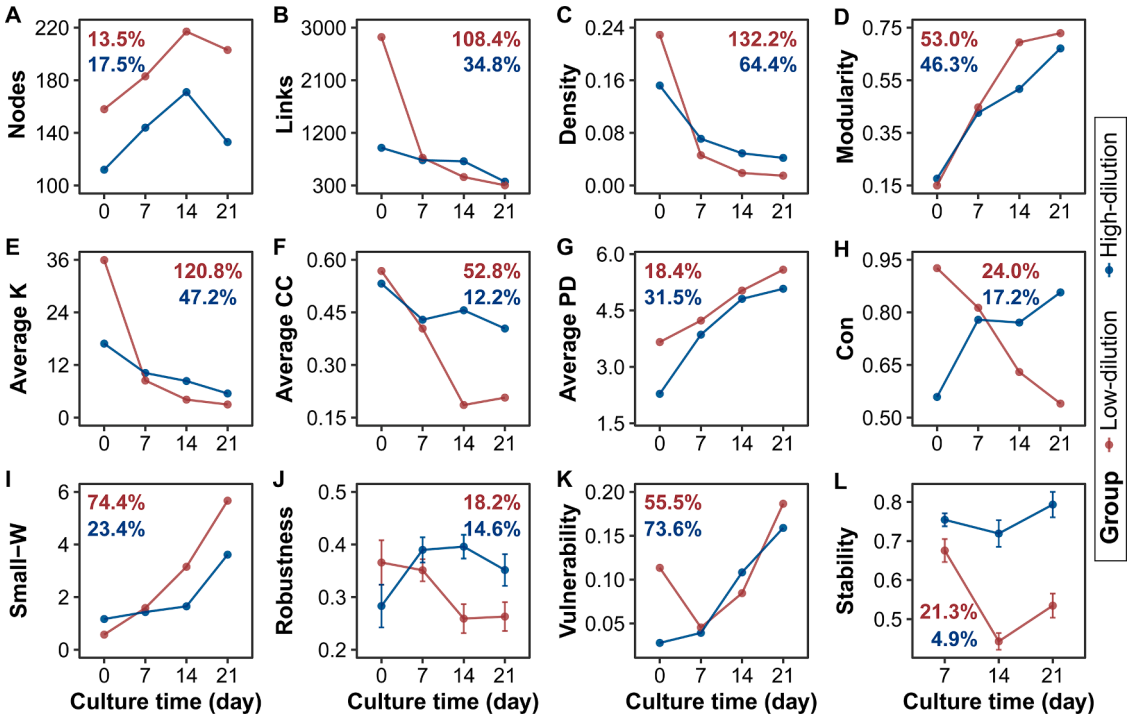

Fig. 5. Temporal changes of MENA network topology and stability in the low- and high-dilution groups. (A) Nodes (total nodes), (B) Links (total links), (C) Density, (D) Modularity, (E) Average K (average degree), (F) Average CC (average clustering coefficient), (G) Average PD (average path distance) and (H) Connectedness were directly calculated by MENA pipelines. (I) Small-W coefficient (small-world coefficient) > 1 indicates "small-world" properties, that is, high interconnectivity and high efficiency. (J) Robustness, the resistance to node loss. The error bar corresponded to the standard deviation of 100 repetitions of the simulation. (K) Vulnerability measured by maximum node vulnerability in each network. (L) Stability, the temporal invariability of community composition from every two adjacent samplings. Each error bar represents the standard deviation in all plots. The red line refers to the low-dilution groups and the blue line to the high-dilution groups. Details of network topological attributes and stabilities are given in Supplementary Table S1. The numbers (percentages) in each plot show the coefficient of variation in the low- (red word) and the high-dilution groups (blue word), respectively.

in a dilution group, Fig. S8), such as Zotu1, Zotu5, Ztou8 or *Fluviimonas*, unclassified Rhizobiaceae and *Raphidiopsis*. This implies that some keystone nodes are similar in the field-collected and lab-cultured communities or between the different treatment groups and that they presumably play a vital role in shaping the respective bacterial communities.

All MENA networks detected, except the network on day 0, were scale free with modular and small-world properties (Fig. 5D, Fig. 5I, Fig. S6, Table S1). This suggests that the organisation of the ecological networks was non-random with profound implications for microbially mediated ecosystem functions and stability. Therefore, species extinction or loss was simulated to calculate the robustness (the resistance to node loss) of each network. On the basis of random species loss, the networks had a lower robustness in the low- than high-dilution groups after day 0 (Fig. 5J, Fig. S9). Furthermore, the network vulnerability was, on average, higher in the low- (0.107 ± 0.060) than in the high-dilution groups (0.084 ± 0.062), and both increased over time (Fig. 5K), indicating that network instability increased in the low-dilution groups with cultivation time.

Multiple stability indices calculated from empirical data supported that the MENA network compositional stability grew weaker in the low-dilution groups. In order 2 (every two adjacent culture time points), the compositional stability of the network community was generally significantly lower ($P < 0.05$) in the low-dilution (0.55 ± 0.12) than in the high-dilution groups (0.76 ± 0.04) (Fig. 5L). In addition, the compositional stability decreased in the low-dilution groups but was constant in the high-dilution groups (Fig. S10A). For orders 3 and 4 (every three and four adjacent culture time points), the compositional stability was always lower in the low-dilution groups than in the high-dilution groups (Fig. S10B-C).

4. Discussion

4.1. Dilution threshold for rare bacterial species in response to *Raphidiopsis raciborskii*

Our experimental approach, involving co-culturing of serially diluted reservoir microorganisms with *R. raciborskii* XM1 in sterilised reservoir water, allowed us to randomly manipulate bacteria species interacting with *R. raciborskii* XM1 in lab cultures. When comparing the results of the different treatments in experiments A and B with each other, *R. raciborskii* XM1 in the D_{0A}, D_{TX}, D_{4A}, D_{5A}, D_{6A} and D_{0B} treatments (high-dilution groups) showed similar growth and photosynthesis trends, whereas the trends varied greatly in the D_{3A}, D_{1B}, D_{2B}, D_{3B}, D_{X1} and D_{X2} treatments (low-dilution groups) over time (Fig. 2). At the same time, we identified great differences in bacterial community composition between the low- and high-dilution groups (Fig. 3). Both experiments indicated that the ≤ 1000-fold dilution level was a threshold for rare bacterial species that inhibited the activity of *Raphidiopsis* in Shidou Reservoir. At values below or above this threshold, the physiology of *R. raciborskii* exhibited significant differences during the 3-week culture studies.

Obviously, dilution altered the α-diversity of the bacterial communities in our culture systems due to the dilution-induced species loss (Fig. S3). Thus, taxonomic species diversity significantly decreased (as expected) in the high-dilution groups compared to the low-dilution groups, while phylogenetic diversity increased. This obvious paradox may be explained by the fact that the high dilution might produce more similar communities as most of the rare species are removed and solely the abundant ones remain. In contrast, the lower dilution steps stochastically reduce some species in the community and thereby increase the dissimilarity between treatments. Recently, a similar pattern has

been traced for soil fungi (Xiong et al., 2021): along the soil-plant continuum, rare fungal taxa showed higher dissimilarity (higher positive phylogenetic diversity), while the abundant taxa were more similar (lower positive phylogenetic diversity). The variations in niche width found in our study were mirrored in that high-dilution levels resulted in a wider niche width and more overlap. (Fig. S4A-B). Consequently, high-dilution levels generated more similar bacterial communities, indicating a more closely related phylogeny and a wider niche of taxa. In addition, niche width did not change with cultivation time in the high-dilution groups but conspicuously decreased in the low-dilution groups (Fig. S4C). This repeats key findings from previous studies demonstrating that the niche width of rare species is much lower than that of abundant ones (Bickel and Or, 2021; Xiong et al., 2021; Xue et al., 2018). Moreover, the neutral community model showed that in the high-dilution groups stochastic processes remained dominant during the entire culture experiment, whereas in the low-dilution groups the stochastic processes weakened in the early stages of the experiment, and deterministic processes became dominant in the late stages (Fig. S5).

4.2. Specific interactions of rare bacterial species and Raphidiopsis raciborskii

Coexisting species often exhibit a negative frequency dependence due to mechanisms that promote population growth and persistence when rare (Wisnoski and Lennon, 2021). Changes in coexistence relationships of rare bacterial species might alter specific interactions, potentially affecting the observed variations in *R. raciborskii* XM1 physiology. We found that the entire bacterial community, separated into six categories, showed different succession patterns over time. In the low-dilution groups, CRT and ART OTU numbers changed most dramatically (Fig. 4), indicating that many rare species quickly responded to the changing environment (Nyirabuhoro et al., 2020; Shade et al., 2014). Although rare bacterial species had a narrow niche width in the low-dilution groups (Fig. S4), they might thrive and become active through cooperative interactions within coexisting communities. Metabolic dependencies can drive species co-occurrence in diverse microbial communities (Zelezniak et al., 2015), and cross-feeding may expand the metabolic niche of bacteria (Garcia et al., 2015; Ona et al., 2021). Also, distinct microbial consortia with specialised metabolic and eco-physiological traits were selected when various phytoplankton exudates were added to the culture (Kieft et al., 2021). In the high-dilution groups, owing to the loss of large numbers of rare species, stable coexistence relationships seemed to be broken. Consequently, the majority of rare species did not change or were lost over time (Fig. 4), suggesting that many of the rare species likely were inactive (Aanderud et al., 2015; Wilhelm et al., 2014) and that the growth of *R. raciborskii* XM1 thus remained unchanged compared to the negative control (Fig. 2). In contrast, in the low-dilution groups, rare bacterial species have the potential to substantially influence the physiological response of *R. raciborskii* XM1 through various specific interactions.

Microbial networks are useful tools to infer the interactions among microbial species. In particular, molecular ecological network analyses (MENAs) show a high robustness against data noise and link network topological properties with environmental factors (Deng et al., 2012). Thus, network topology can mirror interactions between species. Throughout our experiment, in all groups, network complexity declined with time, whereby in the low-dilution groups this change was stronger (Fig. 5B-H, Table S1). Besides, network compositional stability significantly decreased in the low-dilution groups, whereas it remained stable in the high-dilution groups (Fig. 5L, S10). When taking the dynamics of different taxa (Fig. 4) into consideration, the results suggested that in the high-dilution groups the majority of species remained constant, resulting in complex and stable networks, whereas fluctuations in the composition of the rare species led to simpler hierarchical structures and less tight interactions in the low-dilution groups. Moreover, in the low-dilution groups connectedness decreased substantially (Fig. 5H), whereas modularity increased (Fig. 5D) in comparison to the high-dilution groups. This indicated simpler and more fragmented networks in the low- than in the high-dilution groups (Fig. S6). Further, the low-dilution groups generally exhibited higher network vulnerability (Fig. 5K), suggesting that some species in the subcommunity were highly sensitive to environment changes.

Changes in network structure and complexity are closely related to the specific role of individual species. Keystone species, determined on the basis of their within-module connectivity and among-module connectivity, play primary roles in shaping the overall network structure (Banerjee et al., 2018). In the subnetworks, the low-dilution groups had more keystone species, but *R. raciborskii* appeared as a keystone taxon (Zotu5 and Zotu8) solely on day 14 in the high-dilution groups (Fig. S7). This was in line with the observed growth of *R. raciborskii* XM1, which reached maximum biomass in the high-dilution groups around day 14 but minimum biomass in the low-dilution groups (Fig. 2). In the overall-network, *R. raciborskii* appeared as a keystone taxon in the high-dilution groups, while another cyanobacterium, *Cyanobium,* was a keystone taxon in all sample network (Fig. S8). Interestingly, Rhizobiales were the critical keystone taxa in the subnetworks (Zotu120, Zotu1720, Zotu20, Zotu31 and Zotu87; Fig. S7 and Table S2) and the overall network (Zotu467, Zotu790 and Zotu 82; Fig. S8 and Table S3), especially in the low-dilution groups. Rhizobiales are common in freshwater reservoirs and lakes (Kim et al., 2021; Tromas et al., 2017; Zhang et al., 2021), and many of them can fix nitrogen and live in symbioses with other species (Kuypers et al., 2018). It is worth noting that *R. raciborskii* is a diazotrophic cyanobacterium (Huisman et al., 2018). Heterocysts were observed in freshly isolated *R. raciborskii* XM1, but they gradually disappeared after growth in nitrogen-rich medium (i.e. BG11). In the low-dilution groups, where growth of *R. raciborskii* XM1 was inhibited (Fig. 2), it is likely that keystone taxa of Rhizobiales performed nitrogen fixation to maintain the ecosystem stability. In nature, the species Zotu467 (Rhizobiales) occurred as a network connector (nodes linking different modules) (Fig. S8; Table S3), indicating that nitrogen fixation (Tromas et al., 2017) might play a vital role for microbial dynamics and interactions in subtropical deep-water reservoirs. Although *R. raciborskii* and Rhizobiales may have a similar ecological function in terms of nitrogen fixation (i.e. functional redundancy), diversity loss (introduced by dilution) impaired solely the functions of communities with low functional redundancy (i.e. in the high-dilution treatments). In contrast, the functions of bacterial communities with high functional redundancy were unaffected (i.e. in the low-dilution treatments) (Li et al., 2021b). Thus, specialised functions seemed to be sensitive to species diversity, while the broad functions might not be so.

4.3. Functionality of Raphidiopsis raciborskii

Comparative genomics revealed that cyanobacteria have strong habitat adaptation and fitness advantages to organisms in specific environments (Chen et al., 2021; Woodhouse et al., 2016). This is also true for *R. raciborskii*, which is known to tolerate a wide range of temperature and light regimes and has diverse nutritional strategies (Antunes et al., 2015). In our study, *R. raciborskii* XM1 was able to grow quickly in the negative controls (D_{0A} and D_{0B} treatments) under ambient nutrition conditions (Shidou Reservoir water with low nutrient) (Fig. 2). During the first 14 days, *R. raciborskii* grew irrespective of the nutrient limitation from Shidou (low nutrient) and BG11 media (high nutrient). Besides, our strain demonstrated a strong response to nitrogen as its heterocyst disappeared in the nitrogen-rich medium and reappeared in the nitrogen-limited medium of our lab cultures. When co-cultured with the reservoir bacteria community, the growth of this unialgal and xenic strain was inhibited (Fig. 2). Microbiomes associated with alga hosts can regulate between-species interactions and species coexistence relationships and thus alter the host fitness (Grossart et al., 2006, 2005; Grossart and Simon, 2007; Jackrel et al., 2020, 2021). In the initial stage of our experiment, the *R. raciborskii* XM1 biomass gradually increased in all

treatments, but on day 5 or 6 it decreased sharply in the low-dilution groups (Fig. 2), indicating that some bacteria reduced the functionality (i.e. growth) of *R. raciborskii* XM1.

The relative abundance of specific bacteria in the overall community reveals that dilution affects rare and abundant bacterial species in two ways. Abundant species exhibited variable population sizes (quantity effect) in the different treatments, while rare species were either present in low numbers or absent. Both rare and abundant taxa possibly affect the functionality of *R. raciborskii* XM1 (Vico et al., 2021). If abundant, the species influence mainly *R. raciborskii* functionality, and the low-dilution levels should result in stronger inhibition of the cyanobacterium; however, this was not the case, i.e. the effects in the D_{2B} treatment did not differ from those of the D_{3B} treatment (Fig. 2B, Table 1). If rare species primarily influence the functionality, different dilution levels in the low-dilution groups should have similar effects because the presence or absence of rare species should remain unaffected. This notion is supported by our results as the functionality of *R. raciborskii* XM1 was similar in the D_{2B} and D_{3B} treatments. Abundant species have a stronger adaptation potential than rare ones (Liu et al., 2015), and many of them were able to survive and return to higher densities during the 3-week cultivation period. In addition, differences in phylogenetic diversity, niche variations and bacterial community patterns between the low- and high-dilution groups suggest that rare species largely regulate or control the functionality of *R. raciborskii* XM1.

Individuals belonging to the rare subcommunity were either present or absent after dilution, but the overall rare subcommunity still showed a density effect (high density can limit the survival space and intensify species competition). To understand this pattern better, the D_{X1} and D_{X2} treatments were compared to the D_{3B} and D_{0B} treatments (Fig. 1). Overall, the bacterial densities in the D_{3B}, D_{X1} and D_{X2} treatments were similar. Yet, the bacterial community composition in the D_{3B} treatment had higher similarity to the community in the D_{X1} treatment and lower similarity to that of the D_{X2} treatment, while the inhibition effects on *R. raciborskii* in the D_{3B} and D_{X1} treatment were similar (Fig. 2B, Table 1). Although an inhibition effect was also seen in the D_{X2} treatment, it was much weaker than in the D_{3B} and D_{X1} treatments (Table 1). In addition, the standard error of the *R. raciborskii* growth curve (Chl-*a* and OD_{680}) was apparently larger in the D_{X2} treatment than in all the other treatments (Fig. 2B), indicating that differences in community composition (between the D_{X2} and D_{3B} treatments) impacted the growth of *R. raciborskii*. At the same time, changes in bacterial community composition with cultivation time were similar between the D_{3B}, D_{X1} and D_{X2} treatments (Fig. 3B). These results show that the bacterial effects on the functionality of *R. raciborskii* XM1 in the D_{3B} treatment were identical with those in the D_{X1} treatment, but they were stronger than in the D_{X2} treatment, suggesting that differences in community composition rather than in density contributed to the observed stronger inhibition of *R. raciborskii* photosynthesis and growth by rare species in the low-dilution treatments. In summary, our dilution-to-extinction approach revealed a key role of rare bacterial species for bacteria-phytoplankton (i.e. the cyanobacterium *R. raciborskii*) interactions and their related ecological functionality. Consequently, future studies need to take into account the so far largely neglected role of rare bacterial species in explaining the observed changes in the dynamics and ecological role of phytoplankton-bacteria interactions in aquatic ecosystems.

5. Conclusions

We undertook dilution-to-extinction culture experiments together with high-throughput sequencing of 16S rRNA gene amplicons and found that the community composition of rare bacteria demonstrated a more pronounced temporal pattern in the low-dilution groups than in the high-dilution groups. Moreover, rare taxa exhibited strong inhibition of *R. raciborskii* growth and photosynthesis through their mediation of bacterial coexistence and thus functionality. Our findings highlight that the overlooked rare bacterial biosphere might shape the overall functionality of bacterial communities, in particular their interactions with harmful cyanobacteria such as *R. raciborskii*, and has the potential to impact water quality and security. To better understand and mitigate the consequences of harmful algae changes in aquatic ecosystems, more emphasis should be placed on exploring the rare microbial biosphere in a changing environment.

Data availability statement

Raw sequence data were submitted to NCBI (The National center for Biotechnology Information, https://www.ncbi.nlm.nih.gov/) with Sequence Read Archive (SRA) BioProject accession number PRJNA730921 for cultured samples and BioProject accession number PRJNA689332 for field samples.

Author contributions

J.Y. conceived the idea and designed the research. J.Z. and H.H.C. collected the samples. F.J.T. provided the XM1 strain. J.Z. performed the experiments. J.Z. and H.T.Z. sequenced the data. J.Z. and P.X. analysed the data. J.Z. and J.Y. wrote the first draft of the manuscript, H.P.G. and E.J. revised the manuscript, and all authors contributed to and approved the final manuscript.

Declaration of Competing Interest

The authors declare that they have no known competing financial interests or personal relationships that could have appeared to influence the work reported in this paper.

Data availability

Data will be made available on request.

Acknowledgements

Our work was supported by the National Science Foundation of China (32201352, 92251306, 31900093 and 32001152), the Natural Science Foundation of Fujian Province of China (2020J01119 and 2022I0039), the “Fujian STS” Program (2022T3015) of the Chinese Academy of Sciences and the Environmental Protection Science & Technology Project of Fujian Province of China (2021R009). HPG was supported by a grant from the German Science Foundation (DFG, GR 1540/29–1). EJ was supported by WATEC (Centre for Water Technology, AU) and Tübitak BIDEB2232 (Project 118C250).

Supplementary materials

Supplementary material associated with this article can be found, in the online version, at doi:10.1016/j.hal.2022.102350.

References

Aanderud, Z.T., Jones, S.E., Fierer, N., Lennon, J.T., 2015. Resuscitation of the rare biosphere contributes to pulses of ecosystem activity. Front. Microbiol. 6, 24.
Antunes, J.T., Leao, P.N., Vasconcelos, V.M., 2015. *Cylindrospermopsis raciborskii*: review of the distribution, phylogeography, and ecophysiology of a global invasive species. Front. Microbiol. 6, 473.
Banerjee, S., Schlaeppi, K., van der Heijden, M.G.A., 2018. Keystone taxa as drivers of microbiome structure and functioning. Nat. Rev. Microbiol. 16 (9), 567–576.
Bickel, S., Or, D., 2021. The chosen few-variations in common and rare soil bacteria across biomes. ISME J. 15 (11), 3315–3325.
Chen, J., Wang, P.F., Wang, C., Wang, X., Miao, L.Z., Liu, S., Yuan, Q.S., Sun, S.H., 2020. Distinct assembly mechanisms underlie similar biogeographic patterns of rare and abundant bacterioplankton in Cascade reservoirs of a large river. Front. Microbiol. 11, 158.

Chen, M.Y., Teng, W.K., Zhao, L., Hu, C.X., Zhou, Y.K., Han, B.P., Song, L.R., Shu, W.S., 2021. Comparative genomics reveals insights into cyanobacterial evolution and habitat adaptation. ISME J. 15 (1), 211–227.
Chen, W.D., Ren, K.X., Isabwe, A., Chen, H.H., Liu, M., Yang, J., 2019. Stochastic processes shape microeukaryotic community assembly in a subtropical river across wet and dry seasons. Microbiome 7 (1), 138.
Cook, K.V., Li, C., Cai, H.-Y., Krumholz, L.R., Hambright, K.D., Paerl, H.W., Steffen, M. M., Wilson, A.E., Burford, M.A., Grossart, H.P., Hamilton, D.P., Jiang, H.L., Sukenik, A., Latour, D., Meyer, E.I., Padisák, J., Qin, B., Zamor, R.M., Zhu, G.W., 2020. The global *Microcystis* interactome. Limnol. Oceanogr. 65 (S1), S194–S207.
Dee, L.E., Cowles, J., Isbell, F., Pau, S., Gaines, S.D., Reich, P.B., 2019. When do ecosystem services depend on rare species? Trends Ecol. Evol. 34 (8), 746–758.
Deng, Y., Jiang, Y.H., Yang, Y.F., He, Z., Luo, F., Zhou, J.Z., 2012. Molecular ecological network analyses. BMC Bioinformatics 13, 113.
Dick, G.J., Duhaime, M.B., Evans, J.T., Errera, R.M., Godwin, C.M., Kharbush, J.J., Nitschky, H.S., Powers, M.A., Vanderploeg, H.A., Schmidt, K.C., Smith, D.J., Yancey, C.E., Zwiers, C.C., Denef, V.J., 2021. The genetic and ecophysiological diversity of *Microcystis*. Environ. Microbiol. 23 (12), 7278–7313.
Dziallas, C., Grossart, H.P., 2011a. Increasing oxygen radicals and water temperature select for toxic *Microcystis* sp. PLoS ONE 6 (9), e25569.
Dziallas, C., Grossart, H.P., 2011b. Temperature and biotic factors influence bacterial communities associated with the cyanobacterium *Microcystis* sp. Environ. Microbiol. 13 (6), 1632–1641.
Dziallas, C., Grossart, H.P., 2012. Microbial interactions with the cyanobacterium *Microcystis aeruginosa* and their dependence on temperature. Mar. Biol. 159 (11), 2389–2398.
Edgar, R.C., 2010. Search and clustering orders of magnitude faster than BLAST. Bioinformatics 26 (19), 2460–2461.
Edgar, R.C., 2016. UNOISE2: improved error-correction for Illumina 16S and ITS amplicon sequencing. bioRxiv.
Gao, Y., Zhang, W.L., Li, Y., Wu, H.N., Yang, N., Hui, C.Z., 2021. Dams shift microbial community assembly and imprint nitrogen transformation along the Yangtze River. Water Res. 189, 116579.
Garcia, S.L., Buck, M., McMahon, K.D., Grossart, H.P., Eiler, A., Warnecke, F., 2015. Auxotrophy and intrapopulation complementary in the "interactome" of a cultivated freshwater model community. Mol. Ecol. 24 (17), 4449–4459.
Grossart, H.P., Czub, G., Simon, M., 2006. Algae-bacteria interactions and their effects on aggregation and organic matter flux in the sea. Environ. Microbiol. 8 (6), 1074–1084.
Grossart, H.P., Levold, F., Allgaier, M., Simon, M., Brinkhoff, T., 2005. Marine diatom species harbour distinct bacterial communities. Environ. Microbiol. 7 (6), 860–873.
Grossart, H.P., Simon, M., 2007. Interactions of planktonic algae and bacteria: effects on algal growth and organic matter dynamics. Aquat. Microb. Ecol. 47 (2), 163–176.
Hausmann, B., Knorr, K.H., Schreck, K., Tringe, S.G., Glavina Del Rio, T., Loy, A., Pester, M., 2016. Consortia of low-abundance bacteria drive sulfate reduction-dependent degradation of fermentation products in peat soil microcosms. ISME J. 10 (10), 2365–2375.
Herren, C.M., McMahon, K.D., 2018. Keystone taxa predict compositional change in microbial communities. Environ. Microbiol. 20 (6), 2207–2217.
Ho, J.C., Michalak, A.M., Pahlevan, N., 2019. Widespread global increase in intense lake phytoplankton blooms since the 1980s. Nature 574 (7780), 667–670.
Huisman, J., Codd, G.A., Paerl, H.W., Ibelings, B.W., Verspagen, J.M.H., Visser, P.M., 2018. Cyanobacterial blooms. Nat. Rev. Microbiol. 16 (8), 471–483.
Jackrel, S.L., Schmidt, K.C., Cardinale, B.J., Denef, V.J., 2020. Microbiomes reduce their host's sensitivity to interspecific interactions. mBio 11 (1), e02657-19.
Jackrel, S.L., Yang, J.W., Schmidt, K.C., Denef, V.J., 2021. Host specificity of microbiome assembly and its fitness effects in phytoplankton. ISME J. 15 (3), 774–788.
Jia, X., Dini-Andreote, F., Falcao Salles, J., 2018. Community assembly processes of the microbial rare biosphere. Trends Microbiol. 26 (9), 738–747.
Jousset, A., Bienhold, C., Chatzinotas, A., Gallien, L., Gobet, A., Kurm, V., Kusel, K., Rillig, M.C., Rivett, D.W., Salles, J.F., van der Heijden, M.G.A., Youssef, N.H., Zhang, X.W., Wei, Z., Hol, W.H.G., 2017. Where less may be more: how the rare biosphere pulls ecosystems strings. ISME J. 11 (4), 853–862.
Kalaji, H.M., Schansker, G., Ladle, R.J., Goltsev, V., Bosa, K., Allakhverdiev, S.I., Brestic, M., Bussotti, F., Calatayud, A., Dabrowski, P., Elsheery, N.I., Ferroni, L., Guidi, L., Hogewoning, S.W., Jajoo, A., Misra, A.N., Nebauer, S.G., Pancaldi, S., Penella, C., Poli, D., Pollastrini, M., Romanowska-Duda, Z.B., Rutkowska, B., Serodio, J., Suresh, K., Szulc, W., Tambussi, E., Yanniccari, M., Zivcak, M., 2014. Frequently asked questions about in vivo chlorophyll fluorescence: practical issues. Photosynth. Res. 122 (2), 121–158.
Kieft, B., Li, Z., Bryson, S., Hettich, R.L., Pan, C.L., Mayali, X., Mueller, R.S., 2021. Phytoplankton exudates and lysates support distinct microbial consortia with specialized metabolic and ecophysiological traits. Proc. Natl. Acad. Sci. USA 118 (41), e2101178118.
Kim, M.S., Kim, K.H., Hwang, S.J., Lee, T.K., 2021. Role of algal community stability in harmful algal blooms in river-connected lakes. Microb. Ecol. 82 (2), 309–318.
Kuypers, M.M.M., Marchant, H.K., Kartal, B., 2018. The microbial nitrogen-cycling network. Nat. Rev. Microbiol. 16 (5), 263–276.
Lezcano, M.A., Velazquez, D., Quesada, A., El-Shehawy, R., 2017. Diversity and temporal shifts of the bacterial community associated with a toxic cyanobacterial bloom: an interplay between microcystin producers and degraders. Water Res. 125, 52–61.
Li, H., Song, C.L., Yang, L., Qin, H.D., Cao, X.Y., Zhou, Y.Y., 2021a. Phosphorus supply pathways and mechanisms in shallow lakes with different regime. Water Res. 193, 116886.
Li, Y., Ge, Y., Wang, J.C., Shen, C.C., Wang, J.L., Liu, Y.J., 2021b. Functional redundancy and specific taxa modulate the contribution of prokaryotic diversity and composition to multifunctionality. Mol. Ecol. 30 (12), 2915–2930.
Liu, L.M., Yang, J., Yu, Z., Wilkinson, D.M., 2015. The biogeography of abundant and rare bacterioplankton in the lakes and reservoirs of China. ISME J. 9 (9), 2068–2077.
Liu, M., Liu, L.M., Chen, H.H., Yu, Z., Yang, J.R., Xue, Y., Huang, B.Q., Yang, J., 2019. Community dynamics of free-living and particle-attached bacteria following a reservoir *Microcystis* bloom. Sci. Total Environ. 660, 501–511.
Lu, Z., Lei, L.M., Lu, Y., Peng, L., Han, B.P., 2021. Phosphorus deficiency stimulates dominance of *Cylindrospermopsis* through facilitating cylindrospermopsin-induced alkaline phosphatase secretion: integrating field and laboratory-based evidences. Environ. Pollut. 290, 117946.
Lv, H., Yang, J., Liu, L.M., Yu, X.Q., Yu, Z., Chiang, P.C., 2014. Temperature and nutrients are significant drivers of seasonal shift in phytoplankton community from a drinking water reservoir, subtropical China. Environ. Sci. Pollut. Res. 21 (9), 5917–5928.
Mo, Y.Y., Peng, F., Gao, X.F., Xiao, P., Logares, R., Jeppesen, E., Ren, K.X., Xue, Y.Y., Yang, J., 2021. Low shifts in salinity determined assembly processes and network stability of microeukaryotic plankton communities in a subtropical urban reservoir. Microbiome 9, 128.
Mo, Y.Y., Zhang, W.J., Yang, J., Lin, Y.S., Yu, Z., Lin, S.J., 2018. Biogeographic patterns of abundant and rare bacterioplankton in three subtropical bays resulting from selective and neutral processes. ISME J. 12 (9), 2198–2210.
Nyirabuhoro, P., Liu, M., Xiao, P., Liu, L.M., Yu, Z., Wang, L.N., Yang, J., 2020. Seasonal variability of conditionally rare taxa in the water column bacterioplankton community of subtropical reservoirs in China. Microb. Ecol. 80 (1), 14–26.
Olesen, J.M., Bascompte, J., Dupont, Y.L., Jordano, P., 2007. The modularity of pollination networks. Proc. Natl. Acad. Sci. USA 104 (50), 19891–19896.
Ona, L., Giri, S., Avermann, N., Kreienbaum, M., Thormann, K.M., Kost, C., 2021. Obligate cross-feeding expands the metabolic niche of bacteria. Nat. Ecol. Evol. 5 (9), 1224–1232.
Paerl, H.W., Huisman, J., 2008. Blooms like it hot. Science 320 (5872), 57–58.
Perri, K.A., Manning, S.R., Watson, S.B., Fowler, N.L., Boyer, G.L., 2021. Dark adaptation and ability of pulse-amplitude modulated (PAM) fluorometry to identify nutrient limitation in the bloom-forming cyanobacterium, *Microcystis aeruginosa* (Kutzing). J. Photochem. Photobiol. B 219, 112186.
Pester, M., Bittner, N., Deevong, P., Wagner, M., Loy, A., 2010. A "rare biosphere" microorganism contributes to sulfate reduction in a peatland. ISME J. 4 (12), 1591–1602.
Pound, H.L., Martin, R.M., Sheik, C.S., Steffen, M.M., Newell, S.E., Dick, G.J., McKay, R. M.L., Bullerjahn, G.S., Wilhelm, S.W., 2021. Environmental studies of cyanobacterial harmful algal blooms should include interactions with the dynamic microbiome. Environ. Sci. Technol. 55 (19), 12776–12779.
Quast, C., Pruesse, E., Yilmaz, P., Gerken, J., Schweer, T., Yarza, P., Peplies, J., Glöckner, F.O., 2013. The SILVA ribosomal RNA gene database project: improved data processing and web-based tools. Nucleic. Acids. Res. 41, D590–D596.
Ralph, P.J., Gademann, R., 2005. Rapid light curves: a powerful tool to assess photosynthetic activity. Aquat. Bot. 82 (3), 222–237.
Raymond, P.A., Hartmann, J., Lauerwald, R., Sobek, S., McDonald, C., Hoover, M., Butman, D., Striegl, R., Mayorga, E., Humborg, C., Kortelainen, P., Durr, H., Meybeck, M., Ciais, P., Guth, P., 2013. Global carbon dioxide emissions from inland waters. Nature 503 (7476), 355–359.
Rippka, R., Deruelles, J., Waterbury, J.B., Herdman, M., Stanier, R.Y., 1979. Generic assignments, strain histories and properties of pure cultures of cyanobacteria. J. General. Microbiol. 111, 1–61.
Rognes, T., Flouri, T., Nichols, B., Quince, C., Mahé, F., 2016. VSEARCH: a versatile open source tool for metagenomics. PeerJ 4, e2584.
Scarlett, K.R., Kim, S., Lovin, L.M., Chatterjee, S., Scott, J.T., Brooks, B.W., 2020. Global scanning of cylindrospermopsin: critical review and analysis of aquatic occurrence, bioaccumulation, toxicity and health hazards. Sci. Total Environ. 738, 139807.
Schloss, P.D., Westcott, S.L., Ryabin, T., Hall, J.R., Hartmann, M., Hollister, E.B., Lesniewski, R.A., Oakley, B.B., Parks, D.H., Robinson, C.J., Sahl, J.W., Stres, B., Thallinger, G.G., Van Horn, D.J., Weber, C.F., 2009. Introducing mothur: open-source, platform-independent, community-supported software for describing and comparing microbial communities. Appl. Environ. Microbiol. 75 (23), 7537–7541.
Seymour, J.R., Amin, S.A., Raina, J.-B., Stocker, R., 2017. Zooming in on the phycosphere: the ecological interface for phytoplankton-bacteria relationships. Nat. Microbiol. 2, 17065.
Shade, A., Jones, S.E., Caporaso, J.G., Handelsman, J., Knight, R., Fierer, N., Gilbert, J.A., 2014. Conditionally rare taxa disproportionately contribute to temporal changes in microbial diversity. mBio 5 (4), e01371-14.
Sidelev, S., Koksharova, O., Babanazarova, O., Fastner, J., Chernova, E., Gusev, E., 2020. Phylogeographic, toxicological and ecological evidence for the global distribution of *Raphidiopsis raciborskii* and its northernmost presence in Lake Nero, Central Western Russia. Harmful Algae 98, 101889.
Sloan, W.T., Lunn, M., Woodcock, S., Head, I.M., Nee, S., Curtis, T.P., 2006. Quantifying the roles of immigration and chance in shaping prokaryote community structure. Environ. Microbiol. 8 (4), 732–740.
Sogin, M.L., Morrison, H.G., Huber, J.A., Mark Welch, D., Huse, S.M., Neal, P.R., Arrieta, J.M., Herndl, G.J., 2006. Microbial diversity in the deep sea and the underexplored "rare biosphere". Proc. Natl. Acad. Sci. USA 103(32), 12115–12120.
Stegen, J.C., Fredrickson, J.K., Wilkins, M.J., Konopka, A.E., Nelson, W.C., Arntzen, E.V., Chrisler, W.B., Chu, R.K., Danczak, R.E., Fansler, S.J., Kennedy, D.W., Resch, C.T., Tfaily, M., 2016. Groundwater-surface water mixing shifts ecological assembly processes and stimulates organic carbon turnover. Nat. Commun. 7, 11237.

Tan, F.J., Xiao, P., Yang, J.R., Chen, H.H., Jin, L., Yang, Y.G., Lin, T.F., Willis, A., Yang, J., 2021. Precision early detection of invasive and toxic cyanobacteria: a case study of *Raphidiopsis raciborskii*. Harmful Algae 110, 102125.

Te, S.H., Tan, B.F., Thompson, J.R., Gin, K.Y.-H., 2017. Relationship of microbiota and cyanobacterial secondary metabolites in planktothricoides-dominated bloom. Environ. Sci. Technol. 51 (8), 4199–4209.

Tromas, N., Fortin, N., Bedrani, L., Terrat, Y., Cardoso, P., Bird, D., Greer, C.W., Shapiro, B.J., 2017. Characterising and predicting cyanobacterial blooms in an 8-year amplicon sequencing time course. ISME J. 11 (8), 1746–1763.

Vico, P., Iriarte, A., Bonilla, S., Piccini, C., 2021. Metagenomic analysis of *Raphidiopsis raciborskii* microbiome: beyond the individual. Biodivers. Data J. 9, e72514.

Wan, W.J., Grossart, H.P., He, D.L., Yuan, W.K., Yang, Y.Y., 2021. Stronger environmental adaptation of rare rather than abundant bacterioplankton in response to dredging in eutrophic Lake Nanhu (Wuhan, China). Water Res. 190, 116751.

Wang, Y., Ye, F., Wu, S.J., Wu, J.P., Yan, J., Xu, K.Q., Hong, Y.G., 2020. Biogeographic pattern of bacterioplanktonic community and potential function in the Yangtze River: roles of abundant and rare taxa. Sci. Total Environ. 747, 141335.

Wilhelm, L., Besemer, K., Fasching, C., Urich, T., Singer, G.A., Quince, C., Battin, T.J., 2014. Rare but active taxa contribute to community dynamics of benthic biofilms in glacier-fed streams. Environ. Microbiol. 16 (8), 2514–2524.

Wilhelm, S.W., Bullerjahn, G.S., McKay, R.M.L., 2020. The complicated and confusing ecology of *Microcystis* blooms. mBio 11 (3), e00529-20.

Wisnoski, N.I., Lennon, J.T., 2021. Stabilising role of seed banks and the maintenance of bacterial diversity. Ecol. Lett. 24 (11), 2328–2338.

Woodhouse, J.N., Kinsela, A.S., Collins, R.N., Bowling, L.C., Honeyman, G.L., Holliday, J. K., Neilan, B.A., 2016. Microbial communities reflect temporal changes in cyanobacterial composition in a shallow ephemeral freshwater lake. ISME J. 10 (6), 1337–1351.

Xiong, C., He, J.Z., Singh, B.K., Zhu, Y.G., Wang, J.T., Li, P.P., Zhang, Q.B., Han, L.L., Shen, J.P., Ge, A.H., Wu, C.F., Zhang, L.M., 2021. Rare taxa maintain the stability of crop mycobiomes and ecosystem functions. Environ. Microbiol. 23 (4), 1907–1924.

Xue, Y.Y., Chen, H.H., Yang, J.R., Liu, M., Huang, B.Q., Yang, J., 2018. Distinct patterns and processes of abundant and rare eukaryotic plankton communities following a reservoir cyanobacterial bloom. ISME J. 12 (9), 2263–2277.

Yang, J.R., Lv, H., Isabwe, A., Liu, L.M., Yu, X.Q., Chen, H.H., Yang, J., 2017. Disturbance-induced phytoplankton regime shifts and recovery of cyanobacteria dominance in two subtropical reservoirs. Water Res. 120, 52–63.

Yang, Y.M., Yu, G.L., Chen, Y.X., Jia, N.N., Li, R.H., 2021. Four decades of progress in cylindrospermopsin research: the ins and outs of a potent cyanotoxin. J. Hazard. Mater. 406, 124653.

Yuan, M.T.M., Guo, X., Wu, L.W., Zhang, Y., Xiao, N.J., Ning, D.L., Shi, Z., Zhou, X.S., Wu, L.Y., Yang, Y.F., Tiedje, J.M., Zhou, J.Z., 2021. Climate warming enhances microbial network complexity and stability. Nat. Clim. Chang. 11 (4), 343–348.

Zelezniak, A., Andrejev, S., Ponomarova, O., Mende, D.R., Bork, P., Patil, K.R., 2015. Metabolic dependencies drive species co-occurrence in diverse microbial communities. Proc. Natl. Acad. Sci. USA 112 (20), 6449–6454.

Zhang, L.Y., Delgado-Baquerizo, M., Shi, Y., Liu, X., Yang, Y.F., Chu, H.Y., 2021. Co-existing water and sediment bacteria are driven by contrasting environmental factors across glacier-fed aquatic systems. Water Res. 198, 117139.

Zhao, L.P., Zhao, N.S., 2021. Demonstration of causality: back to cultures. Nat. Rev. Gastroenterol. Hepatol. 18 (2), 97–98.

Zhou, J.Z., Deng, Y., Luo, F., He, Z.L., Tu, Q.C., Zhi, X.Y., 2010. Functional molecular ecological networks. mBio 1 (4), e00169-10.

Zhu, L., Wu, Y.L., Song, L.R., Gan, N.Q., 2014. Ecological dynamics of toxic *Microcystis* spp. and microcystin-degrading bacteria in Dianchi Lake, China. Appl. Environ. Microbiol. 80 (6), 1874–1881.

Zhu, L., Zuo, J., Song, L.R., Gan, N.Q., 2016. Microcystin-degrading bacteria affect *mcyD* expression and microcystin synthesis in *Microcystis* spp. J. Environ. Sci. 41, 195–201.

Zuo, J., Hu, L.L., Shen, W., Zeng, J.Y., Li, L., Song, L.R., Gan, N.Q., 2021. The involvement of alpha-proteobacteria *Phenylobacterium* in maintaining the dominance of toxic *Microcystis* blooms in Lake Taihu, China. Environ. Microbiol. 23 (2), 1066–1078.